International Journal of Engineering Sciences & Research Technology

(A Peer Reviewed Online Journal)
Impact Factor: 5.164

IJESRT

RESEARCHERID
THOMSON REUTERS

[Jean* *et al.*, 11(2): February, 2022] ISSN: 2277-9655
IC™ Value: 3.00 Impact Factor: 5.164
CODEN: IJESS7

IJESRT

INTERNATIONAL JOURNAL OF ENGINEERING SCIENCES & RESEARCH TECHNOLOGY

CORRECTION OF A NOISY IMAGE BY A POLYNOMIAL APPROACH AND CHOICE OF THE BEST IMAGE BY ONE OF THE POLYNOMIAL'S ROOTS.

M'boliguipa Jean*, Kradda Ne Koulou Deba*, Oumarou Sanda Abbo*.

* Department of Physics, Faculty of Science, Carnot Energy Laboratory, Central African Republic
(11pt Times New Roman, Center)

DOI: 10.29121/ijesrt.v11.i1.2022.3

ABSTRACT

In this paper a polynomial method of selecting an image disturbed and corrected by the modified power law by one of its roots, is proposed. This power law uses here is a real power variable belonging to the interval [1.00,..1.12]. It provides a dozen corrected images. But it is difficult to get the best image between them, or the image which has the best signal to noise ratio. One of the roots provides this value. Comparison of reconstructed image with the original is proved by structural similarity index (SSIM), entropy and peak signal-to-noise ratio (PSNR) which are objective quality measures and the averages of gray levels of pixels which are very similar. The polynomial selection method has the advantage of providing only a single corrected image without RGB →YCbCr transformation noise and close to original among many others. Where somebody needs to choose one image among several, this method can provide solution.

KEYWORDS: RGB→YCbCr transformation noise, noisy image, signal to noise ratio, polynomial method, polynomial root, corrected image.

1. INTRODUCTION

In the field of improving the quality of an image disturbed by noise, many authors have developed classical improvement methods such as: interpolation method which uses various shapes as described by authors [1-4], histogram equalization method which gives good results in improving color images [5-8] and medical images [9-11]; contrast stretching method which focuses on improving the contrast of an image by "stretching" its range of intensity values to cover a range desired or authorized, presented by the authors [12-13]; compression of the dynamic range [14], partial differential equations method widely used in image filtering and restoration [15-16]; cellular neural networks method known for their success in improving and analyzing medical images [17]; the directional wavelet transformation mainly used for feature extraction, enhancement, denoising, classification and compression [18]. Some methods provide algorithms that apply to areas of an image or its parts all that possess noise. This is for example the method defined by Mingzhou and al. [19] who obtain the classification of images under unfavorable visual conditions using the gray function and the definition function in order to obtain an improvement algorithm of images. Himamshu Singh and al., exploit the advantages of gamma correction and histogram equalization to achieve improvement in dark images [20]. San Chi Liu and al. improved the contrast of an image using an adaptive approach by the Golden Section Search algorithm [21]. The adaptive gamma correction proposed by Gang Cao and al. [22], has improved images with lighter areas and dark areas that often appear in some images after acquisition. P. Jidesh and al, propose a fourth order diffusion filter for the overall enhancement of an image [23]. Thresholded and optimized histogram equalization is a method proposed by P. Shanmugavadivu and al., for image enhancement [24]. It begins by segmenting the histogram of the input image in half using the Otsu threshold [25], on the basis of which a set of weighing constraints is formulated. Then, these constraints are applied to any or both of the sub-histograms relative to the histogram model of the input image. Finally, these two sub-histograms are independently equalized and their union produces a contrast enhanced output image. Lihze and al. talk about removing impulse noise [26]. Classic improvement methods such as the median filter directly manipulate the pixels of the image by moving an odd-sized window on the image support then replacing the central pixel (on which the window is positioned) by the median value of the pixels included in window [27]. As we can see, there are many methods of enhancing images. A method of improving a disturbed image by a mathematical transformation used in the JPEG standard [28] is proposed. The transformation

ISSN: 2277-9655
Impact Factor: 5.164
CODEN: IJESS7

concerned is the RGB→YCbCr one. This image enhancement method is applied to every pixel of disturbed image and exploits the signal-to-noise ratio of this image to be enhanced. The aim is to show how one of the roots of a polynomial can correct an image degraded by using the real-variable power law and provide a corrected image with a high value of the signal-to-noise ratio. This method allows a direct selection of the best image among several corrected images. In this article, the method used to retain the right image is presented first, then the results obtained, discussion will follow before conclusion.

2. MATERIALS AND METHODS

Author [29] has shown that after applying the RGB→YCbCr transformation to certain color images in BMP format, image obtained contains a noise in the form of green dots and distributed randomly over this image. This is called RGB→YCbCr transformation noise. Using a variant of the power law established by W. Pratt [30], the variant proposed uses a real power variable p' such as p' belongs to the interval [1.00 to 1.12] with step 0.01. Thirteen (13) images are obtained showing no noise but with decreasing quality. This is where the so-called polynomial method comes in. After calculating the signal to noise ratios (SNR) of pixels for channels Y, Cb and Cr, one makes the sum of these three values to obtain the sum of SNR or ∑SNR. After, we draw the curve of function ∑SNR = f (p'). Using the polyval() function defined by MATLAB software to provide the corresponding polynomial $g_n(p') = a_n p'^n + ... + a_0 = g(p')$. The roots of the polynomial are calculated. The power law used by [30] uses an integer power variable. This article proposes a real power variable. One of the roots of polynomial is used in the power law to correct the transformed images which must no longer contain the RGB→ YCbCr transformation noise and whose one of these images has greater ∑SNR than the other. It is this image that is close to the original one in terms of quality. The evaluation of the quality of corrected images is done by quality measurements such as the average of the pixels, the root mean square error RMSE, the PSNR [31], the entropy which compares the quantity of information contained in each reconstructed and original images and the structural similarity index SSIM which shows the degree of similarity between the images [32]. The advantage of this image improvement method is that it provides a single value of the power variable p' which correct the noisy image and obtain only one image which has a high value of ∑SNR.

3. RESULTS AND DISCUSSION

3.1 Presentation of the steps

The results are presented as follows: the mathematical transformation RGB→YCbCr is applied to the original image to obtain the transformed and noisy image; the power law with a real power variable p' is applied to the noisy image and thirteen corrected images are obtained; we calculate the signal-to-noise ratio of each corrected image per channel then we add these values to have a table of values of the sum of SNR as a function of p' to obtain the function ∑SNR = f (p'); Matlab's polyval() function provides the corresponding polynomial; the table of roots and their modules are provided and finally, one reconstructed image is retained with the greatest value of ∑SNR.

3.2 Original images

Figure1:

Original Nanie

Figure2:

Original Eamac

Figure3:

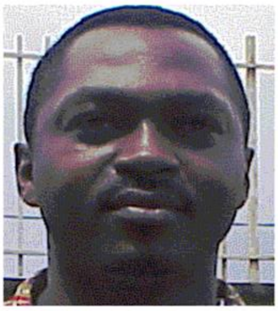

Original Ebala

ISSN: 2277-9655
Impact Factor: 5.164
CODEN: IJESS7

3.3 Transformed and noisy images

Figure4:

Disturbed Nanie

Figure5:

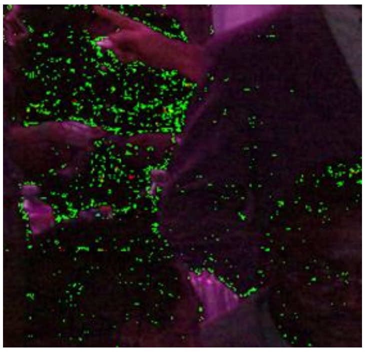

Disturbed Eamac

Figure6:

Disturbed Ebala

Following the application of the RGB→ YCbCr transformation on each image, we observe the transformation noise like green dots distributed randomly on each image. This noise is less dense on Nanie image (Figure4) than on Ebala image (Figure6). It covers the entire Eamac image (Figure 5) which has low contrast.

3.4 Results

3.4.1 Image Nanie.bmp

Table 1: Sum of SNR or ∑SNR values obtained by the real power variable..

P'	1.00	1.01	1.02	1.03	1.04	1.05	1.06	1.07	1.08	1.09	1.10	1.11	1.12
∑SNR	118.97	84.6	64.37	54.06	47.4	43.02	40.13	37.84	35.92	34.29	32.87	31.6	30.48

Figure 7:

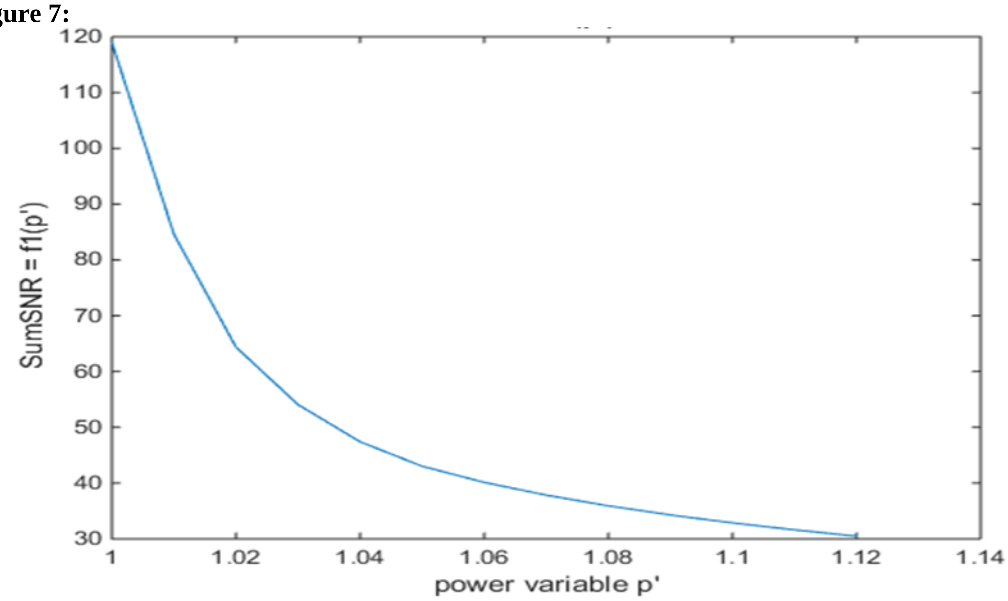

Curve of variation of the Sum of SNR or ∑SNR = $f_1(p')$

In Table 1 and Figure 7, the sum of the SNR decreases with the power variable p'.
Corresponding polynomial:

$$g_1(p') = 1.0e+08*\left(-0.2366p'^5 + 1.2753p'^4 - 2.7491p'^3 + 2.9629p'^2 - 1.5965p' + 0.3441\right)$$

ISSN: 2277-9655
Impact Factor: 5.164
CODEN: IJESS7

Figure 8:

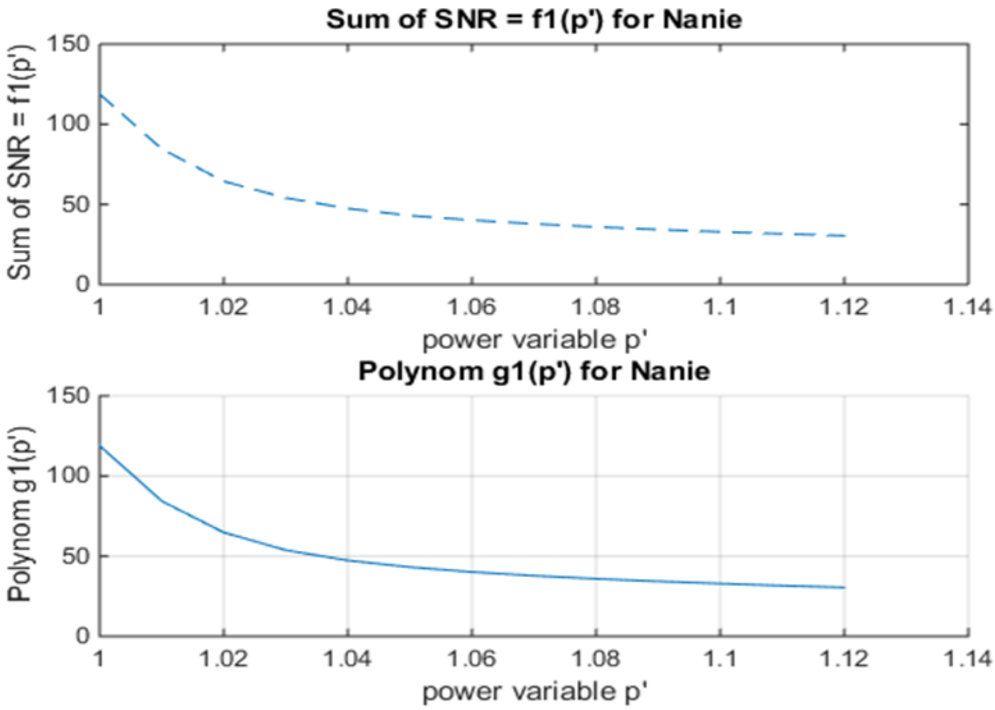

Sum of SNR = $f_1(p')$ and the polynomial $g_1(p')$ for Nanie image.

Table 2: The roots of the polynomial g_1 (p ') and its modules

	Complex roots	Order of roots	Modules of roots
1	1.1490 + 0.0331i	Root3	1.1495
2	1.1490 - 0.0331i		
3	1.0837 + 0.0717i	Root2	1.0861
4	1.0837 - 0.0717i		
5	1.0133 + 0.0466i	Root1	1.0143
6	1.0133 - 0.0466i		

The three images obtained after correction by the power law using these three roots:

Figure 10: **Figure 11:** **Figure 12:**

NanieRoots1 *NanieRoots2* *NanieRoots3*

Sum of SNR: 109.64dB (Root1) 32.52dB (Root2) 24.41dB (Root3)

The three SNR values decrease with the roots values. The larger the root of the polynomial, the more degraded the resulting image. Indeed the image of figure 12 is more degraded than that of figure 10. We note disappearance of the noise.

ISSN: 2277-9655
Impact Factor: 5.164
CODEN: IJESS7

3.4.2 Image Eamac.bmp

Table 3: Sum of SNR or ∑SNR values obtained by the real variable for power law

P'	1.00	1.01	1.02	1.03	1.04	1.05	1.06	1.07	1.08	1.09	1.10	1.11	1.12
∑SNR	73.38	72.59	66.12	59.14	53.21	48.18	43.83	40.09	36.81	33.94	31.42	29.22	27.31

Figure 13:

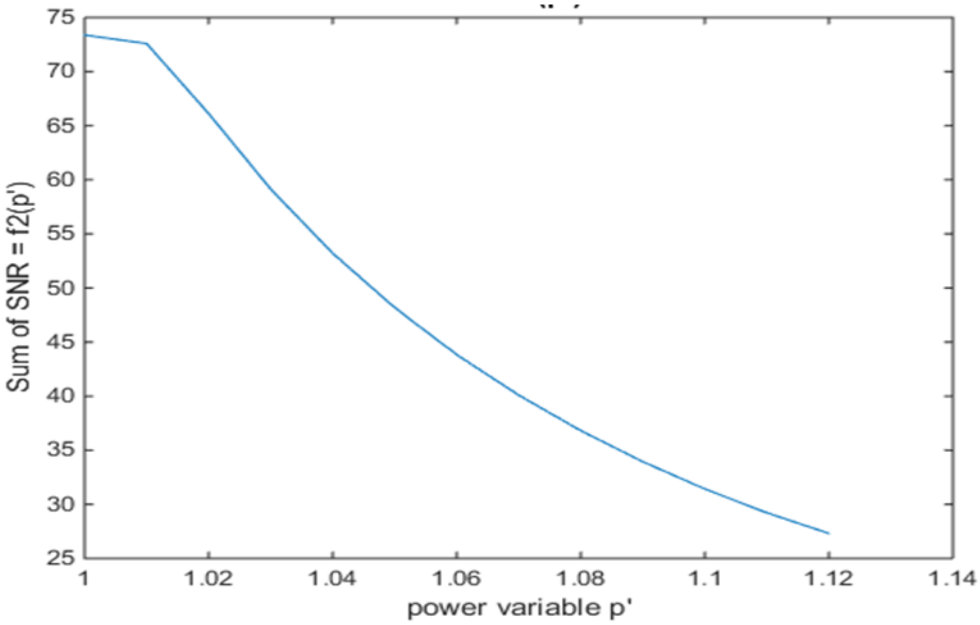

Variation of Sum of SNR or or ∑SNR = f_2(p') for Eamac image.

In Table 3 and Figure 13, the ***∑SNR function*** decreases with the power variable p'.
The corresponding polynomial g_2(p'):

$$g_2(p') = 1.0e+08*\left(0.1667p'^5 - 0.8907p'^4 + 1.9026p'^3 - 2.0312p'^2 + 1.0838p' - 0.2312\right)$$

Figure 14:

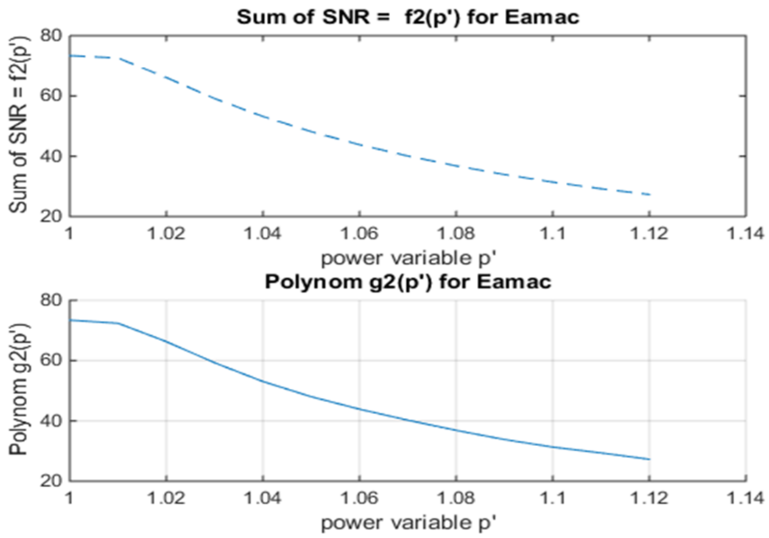

*∑**SNR** = f2(p') and the polynomial g2(p') for Eamac image.*

ISSN: 2277-9655
Impact Factor: 5.164
CODEN: IJESS7

Table 4: The complex roots of the polynomial g2(p) and the corresponding modules:

	Complex roots	Order of roots	Modules of roots
1	1.1341 + 0.0323i	Root3	1.1345
2	1.1341 - 0.0323i		
3	1.0533 + 0.0653i	Root2	1.0554
4	1.0533 - 0.0653i		
5	0.9673 + 0.0000i	Root1	0.9673

The six complex roots provide three real roots.
The three images obtained after applying the power law with the three roots:

Figure 15:

EamacRoot1

Figure 16:

EamacRoot2

Figure 17:

EamacRoot3

Sum of SNR: 45.70dB (Root1) 40.76dB (Root2) 24.94dB (Root3)

The three SNR values decrease with the roots values. The larger the root of the polynomial, the more degraded the resulting image. Indeed, the image of figure 17 is more degraded then for figure 15. We note the disappearance of RGB→YCbCr transformation noise.

3.4.3 Ebala.bmp image

Table 5: Sum of SNR values obtained by the real power variable.

P'	1.00	1.01	1.02	1.03	1.04	1.05	1.06	1.07	1.08	1.09	1.10	1.11	1.12
∑SNR	140.96	99.10	78.13	66.29	58.30	53.29	49.49	45.93	42.79	40.65	38.52	37.15	36.06

Figure 18:

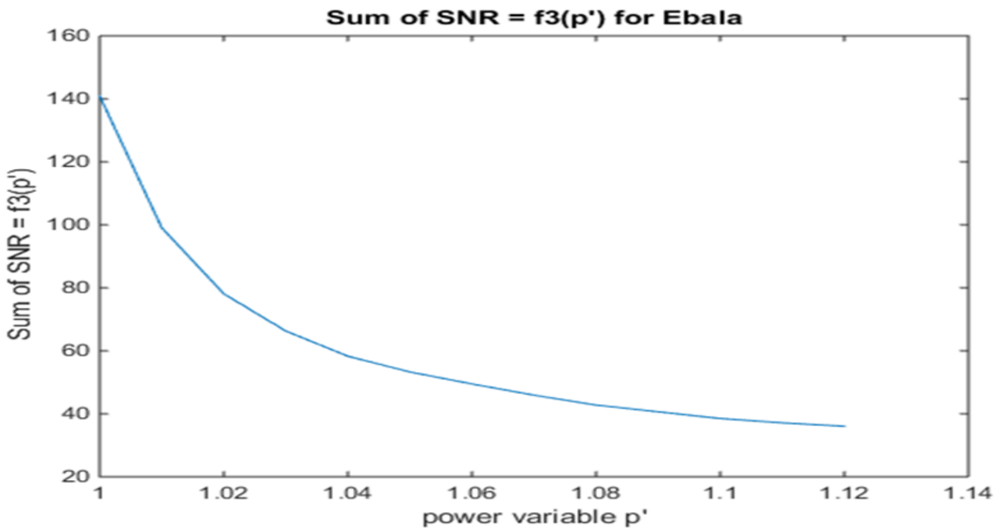

Variation of ∑SNR = f_3 (p')

In Table 4 and Figure 7, the sum of the SNR decreases as a function of the values of the power variable p '.
The corresponding polynomial g_3 (p '):

$$g_3(p') = 1.0e08*\left(-0.3610x^5 + 1.9406x^4 - 4.1720x^3 + 4.4836x^2 - 2.4088x + 0.5176\right)$$

ISSN: 2277-9655
Impact Factor: 5.164
CODEN: IJESS7

Figure 19:

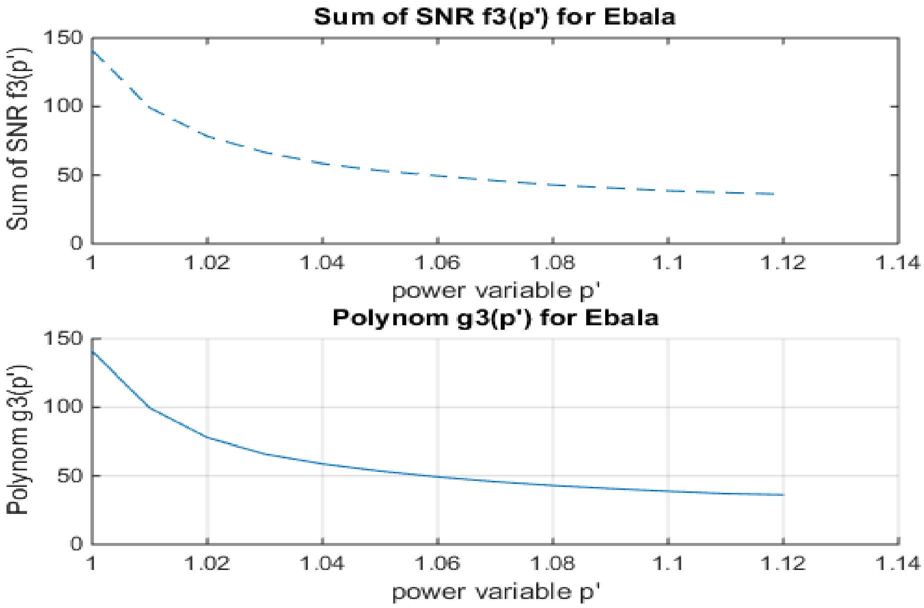

∑SNR = $f_3(p')$ and the polynomial $g_3(p')$ for the Ebala image.

Table 5: The complex roots of the polynomial g_3 (p ') and its real roots

N°	Complex roots	Order of roots	Modules of roots
1	1.1457 + 0.0000i	Root3	1.1457
2	1.0994 + 0.0508i	Root2	1.1006
3	1.0994 - 0.0508i		
4	1.0155 + 0.0436i	Root1	1.0164
5	1.0155 - 0.0436i		

The three images obtained after applying the power law using the values of the three roots of polynomial:

Figure20:

EbalaRoot1

Figure21:

EbalaRoot2

Figure22:

EbalaRoot3

∑*SNR*: 67.52 dB (Root1) 57.39 dB (Root2) 53.80 dB (Root3)

The three values of SNR decrease with the roots. The larger the root of the polynomial is, the more degraded the resulting image is. Indeed, the image of figure 22 is more degraded then which of figure 20. We note the disappearance of the RGB→YcbCr transformation noise.

ISSN: 2277-9655
Impact Factor: 5.164
CODEN: IJESS7

3.4.4 Statistical parameters of original and corrected images.

Table 6: Statistical parameters for Nanie image:

Quality settings		Original image	NanieRoots1 image	Relative errors
Means	Y	120.62	111.93	7%
	Cb	161.29	168.79	4.6%
	Cr	105.55	137.00	29.79%
Entropy	Y	7.48	7.42	0.80%
	Cb	6.07	6.36	4.77%
	Cr	5.49	5.54	0.91%
RMSE	Y	11.05		
	Cb	8.50		
	Cr	38.59		
PSNR (en dB)	Y	27.22		
	Cb	29.47		
	Cr	16.40		
SSIM	Y	0.9904		
	Cb	0.9140		
	Cr	0.9999		

Regarding the average parameters, for Nanie image, it is in the Cr channel that the relative error is high and is close to 30%; for the Y and Cb channels, these relative errors are less than 10%. This shows that the differences between the pixel averages of the original and corrected images are very small in Y and Cb channels. The entropy parameter, which expresses the amount of information in an image, has a relative error less than 5%. This indicates that the difference between the amounts of information in original and corrected images is very small and shows that the two images are almost identical. The structural similarity index (SSIM) between the two images is close to 1, showing how similar the two images are.

Table 7: Statistical parameters for Eamac image:

Quality parameters		Original Image	Image EamacRoot1	Erreur relative
Means	Y	19.79	13.81	30.00%
	Cb	135.09	135.29	00.15%
	Cr	122.49	131.07	07.00%
Entropy	Y	5.52	5.07	08.15%
	Cb	4.04	4.06	00.50%
	Cr	4.14	3.70	10.60%
RMSE	Y	7.92		
	Cb	1.37		
	Cr	13.52		
PSNR (en dB)	Y	30.08		
	Cb	43.49		
	Cr	25.49		
SSIM	Y	0.8677		
,	Cb	0.9522		
	Cr	0.9740		

For Eamac image, it is in the Y channel that the relative error on the means is high (30%); but for Cb and Cr channels, these relative errors are less than 10%. This shows that the differences between the averages of the pixels of the original and corrected images are very small in the Cb and Cr channels. The entropy values have a variable relative error per channel. This error is of the order of 10% in the Cr channel, but less than 10% in the Y and Cb channels. This indicates that the difference between the amounts of information in the original image and the reconstructed image is small and shows that the two images are almost identical. The structural similarity index (SSIM) between the two images is close to unit 1, showing how similar the two images are.

ISSN: 2277-9655
Impact Factor: 5.164
CODEN: IJESS7

Table8: Statistical parameters for Ebala image:

Quality parameters		Original image	EbalaRoot1 Image	Relative Error
Means	Y	145.87	149.10	02.20%
	Cb	129.10	129.39	00.22%
	Cr	130.22	128.00	01.70%
Entropy	Y	3.66	3.65	01.00%
	Cb	2.10	2.95	00.40%
	Cr	2.19	2.96	26.10%
RMSE	Y		11.28	
	Cb		6.03	
	Cr		33.48	
PSNR (en dB)	Y		27.04	
	Cb		32.39	
	Cr		17.62	
SSIM	Y		0.9957	
	Cb		0.9863	
	Cr		0.8997	

For the Ebala image, the relative errors on the means are very small and less than 5%. There are no big differences between the original image and the reconstructed image in terms of the gray levels average values. Regarding the entropy values, it is only in the Cr channel that the relative error exceeds 25%. In the other Y and Cb channels, these errors are less than 5%. The similarity index values between the two images are close to unity, thus showing the great resemblance between the original image and the reconstructed image.

3-5 Discussion

Applying the RGB→YCbCr transformation to each of the three images effectively provided images which are disturbed by the noise called RGB→YCbCr transformation noise as shown in Figures 4, 5 and 6. Tables 1, 3 and 5 contain the values of the sums of the signal to noise ratios which make it possible to obtain Figures7,13,18 which represent the curves of the functions Sum of SNR = fi (p') with i = 1, 2 and 3.

These figures clearly show that the sums of the signal to noise ratios decrease with the real power variable. The variations of the polynomials g_i (p') with i = 1, 2 and 3 in Figures 7, 8, 13, 14, 18 and 19 are identical to the variations of the functions Sum of SNR = fi (p'). The polynomials therefore fully reproduce the variations of the functions Sum of SNR = fi (p'). The modules of the complex roots of the polynomials make it possible to obtain three images with different signal-to-noise ratios (see Figures 10, 11, 12-15, 16, 17-20, 21, 22). The values of the signal-to-noise ratios obtained by applying the real power variable decrease when real variable increases. Indeed, as one approaches the large value of the power variable, the image deteriorates more and more and then evolves towards low values of the signal-to-noise ratio. The Figures (10, 11, 12 - 15, 16, 17 - 20, 21, 22) obtained confirm this result. The latter is also confirmed by variation of corresponding polynomial function. This curve contains the values of the Sum of SNRs as a function of the real power variables among which are the roots of the polynomial. The smallest value of the roots of this polynomial gives an image of better quality and high value of signal-to-noise ratio. This is valid for the three images studied. Quality measurements which are means values of the pixels' gray levels, entropy, signal to noise ratio (see Tables 6, 7 and 8) provide values which show small difference between original and corrected image by the smallest root of the polynomial. Thus, polynomial method makes possible to provide three roots, then the smaller provides an image of best quality and close to the original. The calculated quality measurements are closer to that of the original image than those provided by the larger roots. The interest of this work is that, this polynomial method makes possible the selection of the best quality image among several others in the case that a choice must be made.

4. CONCLUSION

The work carried out in this article concerns the correction followed by the selection of an image disturbed by the mathematical transformation RGB→YCbCr and corrected by the smallest root of a polynomial. The noise caused by this transformation appears in the form of green grains and is distributed randomly over the images used.

The correction of this noise is made by a real power variable of the power law belonging to an interval containing 13 values. These values provide 13 values of decreasing signal-to-noise ratio values. The polynomial

ISSN: 2277-9655
Impact Factor: 5.164
CODEN: IJESS7

corresponding to this function effectively provides a root which gives an image without noise and having a high signal-to-noise ratio value, therefore closer to the original image. This method offers the advantage of selecting one image among several if necessary, and is added to the panoply of improving contrast methods and correcting certain specific noises.

5. ACKNOWLEDGEMENTS

We would like to thank the colleagues from the Carnot Energy Laboratory who kindly took part in this work, which did not require funding.

REFERENCES

[1] Parth Bhatt, Ankit Shah, Sachin Patel, Sanjay Patel,"Image Enhancement Using Various Interpolation, Methods, in International Journal of Computer Science and Information Technology & Security (IJCSITS). 2012; Vol.2: N°4.
[2] Harikrishna O, Maheshwari A., "Satellite image resolution enhancement using dwt technique" in International Journal of Soft Computing and Engineering. 2012;2:5.
[3] Paul Cockshott W, Sumitha L. Balasuriya, Irwan Prasetya Gunawan, Paul Siebert J., "Image enhancement using vector quantisation-based interpolation, in Proceedings of the British Machine Vision Conference, University of Warwick; 2007.
[4] Jagadeesh P., "Image resolution enhancement based on edge directed interpolation using dual tree-complex wavelet", in Proceedings of International Conference on Recent Trends in Information Technology, 3-5 June Chennai, Tamil Nada. 2011; 759-763.
[5] Nikoletta Bassiou, Constantine Kotropoulos., "Color Image histogram equalization by absolute discounting back-off", in Computer Vision and Image Understanding. 2007; 107:108–122.
[6] Kai-Qi Huang, Qiao Wang, Zhen-Yang Wu.,"Natural color image enhancement and evaluation algorithm based on human visual system" in Computer Vision and Image Understanding. 2006; 103:52–63.
[7] Sim KS, Tso CP, Tan YY., "Recursive sub-image histogram equalization applied to gray scale images", in Pattern Recognition Letters. 2007; 28:1209–1221.
[8] Bonghyup Kang, Changwon Jeon, David K. Han, Hanseok Ko., "Adaptive height-modified histogram equalization and chroma correction in ycbcr color space for fast backlight image compensation", in Image and Vision Computing. 2011; 29:557–568.
[9] Francois Pitie, Anil C. Kokaram, Rozenn Dahyot., "Automated colour grading using colour distribution transfer", in Computer Vision and Image Understanding. 2007; 107:123–137.
[10] Soong-Der Chen, Abd. Rahman Ramli., "Preserving brightness in histogram equalization based contrast enhancement techniques", in Digital Signal Processing. 2004; 14:413–428.
[11] Jaspreet Kaur, Amita Choudhar,."Comparison of several contrast stretching techniques on acute leukemia images", in International Journal of Engineering and Innovative Technology (IJEIT). 2012;2:1.
[12] Sos Agaian, Blair Silver, Karen Panetta, "Transform Coefficient Histogram Based Image Enhancement Algorithms using Contrast Entropy", in IEEE TIP-01692-2007.
[13] Chi-Yi Tsai, Chien-Hsing Chou," A novel simultaneous dynamic range compression and local contrast enhancement algorithm for digital video cameras", in EURASIP Journal on Image and Video Processing. 2011;
[14] Zhouchen Lin, Wei Zhang, Xiaoou Tang," Designing Partial Differential Equations for Image Processing by Combining Differential Invariants" in Microsoft Technical Report, MSR-TR-2009-192, 2009.
[15] Nadernejad Ehsan, Hamidreza Koohi, Hamid Hassanpour. "PDEs-Based Method for Image Enhancement", in Applied Mathematical Sciences. 2008; 2(20):981-993.
[16] Aizenberga I, Aizenberga N, Hiltnerb J, Moragab C, Meyer zu Bextenc E., "Cellular neural networks and computational intelligence in medical image processing", in Image and Vision Computing. 2001; 19:177–183.
[17] Yue Lu, Minh N. Do,"The finer directional wavelet transform», Unpublished, Available on http://www.ifp.illinois.edu/~ minhdo/publications/fdw_icassp.pdf.

ISSN: 2277-9655
Impact Factor: 5.164
CODEN: IJESS7

[18] Mingzhou LIU; Qiannan JIANG; Jing HU, "Detection of highway lane lines and drivable regions based on dynamic image enhancement algorithm under unfavorable vision", in Computers & Electrical Engineering (IF 2.663) , DOI: 10.1016/j.compeleceng.2020.106911

[19] Himanshu Singh, Kumara , L.K. Balyanb , G.K. Singh , "Swarm intelligence optimized piecewise gamma corrected histogram equalization for dark image enhancement", in Computers and Electrical Engineering journal homepage, 2017, 1–14, www.elsevier.com/locate/compeleceng.

[20] San Chi Liu[a] Shilong Liu[a] HongkunWu[a] MdArifur Rahman[a] StephenChing-Feng Lin[a] Chin Yeow Wong[a] NgaimingKwok[a] HaiyanShi[b] , "Enhancement of Low Illumination Images based on an Optimal Hyperbolic Tangent Profile", in Computers & Electrical Engineering; Volume 70, August 2018, Pages 538-550

[21] Gang Cao, Lihui Huang, Huawei Tian, Xianglin Huang, Yongbin Wang, Ruicong Zhi, "Contrast Enhancement of Brightness-Distorted Images by Improved Adaptive Gamma Correction Subjects", in Computer Vision and Pattern Recognition (cs.CV).

[22] Nazeer Muhammad, Nargis Bibi, Abdul Wahab Zahid, Mahmood Tallha Akram, Syed Rameez Naqvi, Hyun Sook Oh[f] Dai-Gyoung Kim, "Image de-noising with subband replacement and fusion process using bayes estimators, in Computers & Electrical Engineering Volume 70, August 2018, Pages 413-427 https://doi.org/10.1016/j.compeleceng.2017.05.023

[23] P. Shanmugavadivu[a] K.Balasubramanian, "Thresholded and Optimized Histogram Equalization for contrast enhancement of images", in Computers & Electrical Engineering ; Volume 40, Issue 3, April 2014, Pages 757-768; https://doi.org/10.1016/j.compeleceng.2013.06.013

[24] N. Otsu, "*A threshold selection method from grey scale histogram"*, in IEEE Trans. on Syst. Man and Cyber., vol 1, pp 62-66, 1979

[25] YantaoWang, HaoranLiu, DaliangWang, DaweiLiu ,"Image processing in fault identification for power equipment based on improved super green algorithm", in Computers & Electrical Engineering ; ; Volume 87, October 2020, 106753. https://doi.org/10.1016/j.compeleceng.2020.106753

[26] Lizhe Tan, Jean Jiang, '' Median filter'', in Digital Signal Processing (Third Edition), 2019

[27] Huynh-Thu,Q. et al., ''Scope of validity of PSNR in image/video quality assessment ', in *Electronics Letters* (2008),44(13):800 : http://dx.doi.org/10.1049/el:20080522.

[28] Hamilton E. JPEG File Interchange Format, version 1.02, September 1.

[29] M'Boliguipa, J., Tonyé, E., Nanci Yossi, R., ''Nouvelle méthode de restauration d'images photographiques en couleur dégradées par le bruit de la transformation RGB→YCbCr'' in *Ann. Télécommun.* **61,** 489–516 (2006). https://doi.org/10.1007/BF03219919.

[30] Pratt W.K., ''Digital image processing'', in A Wiley-Interscience Publication, John Wiley-Sons.

[31] https://en.wikipedia.org/wiki/Peak_signal-to-noise_ratio

[32] Z. Wang, A. C. Bovik, H. R. Sheikh and E. P. Simoncelli, "Image quality assessment: From error visibility to structural similarity," in *IEEE Transactions on Image Processing*, vol. 13, no. 4, pp. 600-612, Apr. 2004.